

1 **Supplementary Materials for**

2 **A revisit on the enhancing effect of Tween-80 on the bioremediation of**

3 **PAH-contaminated soil with a surfactant-compatible strain**

4
5 Likun Zhao ^a, Rui Yue ^{a,b}, Hua Li ^a, Shiyu Bao ^a, Chaoqi Chen ^{a,*}, Kaihong Chen ^a, Jin Qi
6 ^a, Xuhui Mao ^{a,*}

7
8 ^a School of Resource and Environmental Sciences, Hubei International Scientific and
9 Technological Cooperation Base of Sustainable Resource and Energy, Wuhan University,
10 Wuhan 430079, China

11 ^b No. 208 Hydrogeological and Engineering Geological Team, Chongqing Bureau of
12 Geological and Mineral Resource Exploration and Development, Chongqing, 400700,
13 China

14
15 * Corresponding Authors: clab@whu.edu.cn (X. Mao); chenchaoqi@whu.edu.cn (C.
16 Chen)

17

18 **Contents**

19 **Text S1.** The preparation of MSM and double-layer agar plates.

20 **Text S2.** The preparation procedure for the inoculation of strain DH-6.

21 **Text S3.** Extraction of PAHs in liquid and solid phases.

22 **Text S4.** Conditions of the HPLC system.

23 **Text S5.** Testing steps for determining the contribution of biosorption.

24 **Text S6.** Quantitative PCR analysis of functional genes.

25 **Text S7.** Identification of intermediates of PAHs.

26 **Text S8.** Test procedure for seed germination and plant growth.

27 **Text S9.** Fenton oxidation of PAH-contaminated field soil.

28 **Table S1.** Physicochemical properties of the spiked soil and the contaminated field soil.

29 **Table S2.** Initial concentrations of PAHs and dosages of Tween-80 in the liquid medium.

30 **Table S3.** Initial concentrations of PAHs in the contaminated field soil.

31 **Table S4.** Detected intermediates of PAHs in the bioremediation process.

32 **Table S5.** Comparison of this study with the literatures concerning the bioremediation of

33 PAHs in liquid media with Tween-80.

34 **Table S6.** Comparison of this study with the literatures concerning the bioremediation of

35 PAH-contaminated field soil with Tween-80.

36 **Fig. S1.** The lab-scale slurry bioreactor used in this study.

37 **Fig. S2.** (a) Appearance of the formed colonies, (b) TEM image of strain DH-6, and (c)

38 phylogenetic relationships of strain DH-6.

39 **Fig. S3.** Removal efficiency of (a) Σ PAHs and five spiked PAHs in (b) liquid phase and
40 (c) solid phase on day 21.

41 **Fig. S4.** (a) Linear relationship between the solubilization of Pyr and its removal
42 efficiency. (b) OD_{600} of strain DH-6 in the MSM supplemented with 100 mg/L of Pyr and
43 different concentrations of Tween-80. FCM analysis of strain DH-6 in PS (c) and PT (d)
44 during the logarithmic growth phase (36 h).

45 **Fig. S5.** Results of the microbial activity analysis on strain DH-6 in PS (a-c) and PT (d-f)
46 during the logarithmic growth phase (36 h).

47 **Fig. S6.** Removal efficiency of (a) Nap, (b) Phe, (c) Flu, (d) Pyr, (e) BaA, (f) BbF, (g)
48 BaP, (h) DBahA in the MSM treated with DH-6, and (i) average removal efficiencies of
49 PAHs on day 7. The symbol “ Φ ” represents the removal efficiencies.

50 **Fig. S7.** QPCR of functional genes related to degrading PAHs in strain DH-6.

51 **Fig. S8.** pH variations for the contaminated field soils that were subjected to different
52 treatments.

53 **Fig. S9.** The pilot-scale equipment for the experiments on the PAH-contaminated field
54 soil.

55

56 **Text S1. The preparation of MSM and double-layer agar plates.**

57 The mineral salt medium (MSM) was prepared with KH_2PO_4 (1.7 g/L),
58 $\text{K}_2\text{HPO}_4 \cdot 3\text{H}_2\text{O}$ (5.6 g/L), NH_4Cl (1.0 g/L), NaCl (0.5 g/L), MgSO_4 (100 mg/L),
59 $\text{MnSO}_4 \cdot \text{H}_2\text{O}$ (20 mg/L), $\text{FeSO}_4 \cdot 7\text{H}_2\text{O}$ (10 mg/L), and CaCl_2 (15 mg/L).

60 The overlayer and underlayer of agar plates were prepared separately. MSM
61 containing 1% agar and 1.5% agar was sterilized at 121°C for 20 min, respectively. The
62 MSM containing 1.5% agar was poured onto sterilized plates (diameter of 90 mm) to
63 form the underlayer. In addition, 0.2 mL of acetone containing 8 mg/mL of Pyr was added
64 to MSM containing 1% agar. The mixture was set for 5-10 min to allow the volatilization
65 of acetone and poured onto the underlayer to form the overlayer. The final concentration
66 of Pyr in the overlayer of the agar plates was 400 mg/L.

67 **Text S2. The procedure for the inoculation of strain DH-6.**

68 Before inoculation, the strain DH-6 was enriched in LB broth and collected in the
69 logarithmic phase. The cells were harvested by centrifuging at 5000 rpm for 5 min,
70 washed three times, and resuspended using MSM solution. The cell density was adjusted
71 to an optical density of 1.0 at a wavelength of 600 nm (OD_{600}). The suspension was then
72 incubated at 30°C for 2 hours before being added to the slurry.

73 **Text S3. Extraction of PAHs in liquid and solid phases.**

74 The extraction method for PAHs in the liquid phase is as follows: briefly, 300 μL of
75 the sample was mixed with 900 μL n-hexane in a 2 mL centrifuge tube, shaken vigorously
76 for 10 min, and centrifuged at 12000 rpm for 10 min at 37°C. Approximately 400 μL of
77 supernatant was filtered to the analytical vial, and measured by high-performance liquid
78 chromatography (HPLC).

79 The extraction method for PAHs in the solid phase is as follows: firstly, take a 2 g

80 soil sample and add 10 mL n-hexane solution. Vortex mix the mixture for 15 min and
81 perform ultrasonic extraction for 30 min. Then, centrifuge the mixture at 5000 rpm for 10
82 min and collect the extraction solution. Repeat the extraction process once and combine
83 the two extraction solutions. Add a suitable quantity of anhydrous sodium sulfate and
84 copper powder, vortex mix for 5 min, then nitrogen blow-off to a volume of 0.5 mL, and
85 adjust the volume to 1 mL with n-hexane. Next, purify the sample using a column filled
86 with magnesium silicate to remove impurities. Elute the column with 10 mL of elution
87 solvent (dichloromethane: n-hexane = 1:1, v/v), collect the eluate, and then evaporate the
88 solvent using a stream of nitrogen gas until the volume reduces to 0.5 mL. Finally, adjust
89 the volume to 1 mL with n-hexane, and measured by HPLC.

90 **Text S4. Conditions of the HPLC system.**

91 Conditions of high-performance liquid chromatography (HPLC, Shimadzu) system
92 were as follows: C18 column (4.6 ×150 mm), column temperature (35°C), flow rate (1
93 mL/min), mobile phase (water: methanol = 10:90), injection volume (20 μL), and
94 detection wavelength (254 nm). All established standard curves had $R^2 > 0.999$. The
95 concentrations of PAHs were determined from peak areas at corresponding retention
96 times.

97 **Text S5. Testing steps for determining the contribution of biosorption**

98 The total removal efficiency of PAHs by strain DH-6 is composed of decay,
99 biodegradation and biosorption. Firstly, the sample collected at “t” time was divided into
100 two parts. The one part was centrifuged at 5000 rpm for 5 minutes, and the PAHs content
101 in the supernatant was tested as C_{t1} . The other part was sonicated for 10 minutes in an ice
102 bath to ensure the lysis of DH-6 cells, and the PAHs content was tested as C_{t2} . Secondly,
103 the total removal efficiency (Φ) of PAHs was calculated using the equation $\Phi = (1 - C_{t1}/C_0)$

104 $\times 100\%$, where C_0 is the initial concentration of PAHs. Finally, the biosorption efficiency
105 (Φ_a) of PAHs was calculated using the equation $\Phi_a = \Phi - (1 - C_{t2}/C_0) \times 100\%$.

106 **Text S6. Quantitative PCR analysis of functional genes.**

107 The strain DH-6 was cultured in the negative control medium (MSM with 10 g/L
108 Tween-80) and the experimental medium (MSM with 10 g/L Tween-80 and 100 mg/L
109 Pyr), respectively. The sampling time of RNA extraction was designed according to
110 degradation curves of Pyr in each of treatments. The RNA was sequenced by on Illumina
111 sequencing platform using Next-Generation Sequencing (NGS). The rpsL was regarded
112 as a reference gene. The fold change in gene expression was calculated by $2^{-\Delta\Delta Ct}$. The
113 program primers of each genes are listed below.

114 pcaG-F: GCGGCATCAACATCCACTTG.

115 pcaG-R: AAACGGTAGGCGAGCTGTC.

116 pcaH-F: GACCTGCTGCTCAACTTCG.

117 pcaH-R: AGGTAGCGGTCGTTCTTGTG.

118 ligA-F: CGCTTCATCTTCGCTCTGG.

119 ligA-R: CGGCAGGTAGGTCAACACT.

120 flnD2-F: CTCCAGAACCGCAACAACCT.

121 flnD2-R: AGCATCGCAGCACCTTCAG.

122 phtAb-F: GTGACCAACGCGATTTCCG.

123 phtAb-R: GAAGCCACCGAACACATTGAC.

124 mobA-F: CCGCAACCAGGAACGCTAT.

125 mobA-R: AGCAGGGTTTCCAGCAAGG.

126 rpsL-F: GCAAGCGCATGGTCGACAAGA.

127 rpsL-R: CGCTGTGCTCTTGCAGGTTGTGA.

128 **Text S7. Identification of intermediates of PAHs.**

129 The degradation intermediates of PAHs were extracted using liquid-liquid extraction.
130 Briefly, 20 mL of samples were adjusted to $\text{pH} < 2$. The samples were then sonicated for
131 10 minutes in an ice bath to ensure the lysis of DH-6 cells. Samples were mixed with 20
132 mL ethyl acetate. The extraction was repeated and the extracts were dewatered using
133 sodium sulfate anhydrous. The extracts were further concentrated by nitrogen sweeping.

134 The extract was analyzed using a Liquid Chromatography High Resolution Mass
135 Spectrometer (LCHRMS, a shimadzu prominence UFLC-20A system (Shimadzu
136 Corporation, Kyoto, Japan) coupled with a quadrupole time-of-flight mass spectrometer
137 (Ab sciex Triple QTOF5600+, AB Sciex, Redwood, CA, USA)) and a Gas
138 Chromatography-Mass Spectrometry (GC-MS, Agilent & GC-7890A; MS-5975C, USA).

139 For LCHRMS, the chromatographic column was Hypersil GOLD C18 column (2.1
140 \times 100 mm, 3 μm pore size, Thermo). The mobile phase consisted of water and acetonitrile,
141 and the flow rate was set at 0.3 mL/min. The injection volume was 10 μL . The mass
142 spectrometer includes an electrospray ionization (ESI) source. The Ion Source Gas1 was
143 set at 55 psi, Ion Source Gas2 at 60 psi, and the Curtain Gas at 30 psi. The temperature of
144 the system was maintained at 550°C. The IonSpray Voltage was set to float between -
145 4500V and 5500V. The Declustering Potential was set at 80V, and the Collision Energy
146 was set at 35V with a Collision Energy Spread of 15V. The analysis was performed in the
147 m/z range of 100 to 1000. The analysis was performed in the negative ion mode using
148 Time-of-Flight Mass Spectrometry (TOF-MS), and ten TOF-MS/MS data sets were
149 collected. The data acquisition was carried out using the information-dependent
150 acquisition (IDA) function.

151 For GC-MS, the extracts were incubated with an equal volume of 99% BSTFA + 1%

152 TMCS before injection. The chromatographic column used was HP-5MS (30.0m×250μm,
153 0.25μm). The initial temperature was set at 60°C for 3 minutes, then ramped at a rate of
154 20°C /min to 180°C and held for 5 minutes, followed by a ramp of 10°C/min to 300°C
155 and held for 5 minutes. The injector temperature was 280°C. The transfer line temperature
156 was 300. Helium was used as the carrier gas with a flow rate of 1.0 mL/min. Splitless
157 injection mode was employed, and the injection volume was 1 μL. The mass spectrometry
158 includes an electron ionization (EI) source with an electron energy of 70 eV. The ion
159 source temperature was 230°C and the quadrupole temperature was 150°C. The scan
160 mode was used with a scan range for mass ranging from 35 to 600.

161 **Text S8. Test of seed germination and plant growth.**

162 Briefly, 100 g of freeze-dried soil was added to each plate (diameter of 90 mm). In
163 each plate, 30 wheat seeds (*Triticum aestivum* L., obtained from the Beijing Academy of
164 Agriculture and Forestry Sciences, China.) were sowed. The plates were incubated in the
165 dark/light cycle (14/10 h) at 25 ± 1°C. The moisture was maintained at 60% by watering
166 every day. In addition, the untreated soil was used as a control. All experiments were
167 conducted in replicates. The numbers of germinated seeds on day 1, day 3, and day 5 were
168 counted manually, respectively. On day 5, the soil was separated from plants by soaking
169 in sterilized water for 5 min. The stem and roots were carefully separated using a sterilized
170 scissor. The stem length and root length were measured manually. The stem and roots
171 were oven-dried at 105°C to constant weight before being weighed.

172 **Text S9. Fenton oxidation of PAHs in the contaminated field soil.**

173 The Fenton oxidation of PAHs was also examined in a slurry bioreactor. In the
174 reactor, 0.1 kg of the contaminated field soil was mixed with 0.9 L of MSM (with 10 g/L
175 Tween-80). Subsequently, a pre-reaction was conducted for 1 hour at 30°C and 200 rpm

176 to enhance the solubility of PAHs in the solution. In the slurry reactor, solutions of ferrous
177 sulfate (FeSO_4) and hydrogen peroxide (H_2O_2) were separately added to ensure that the
178 concentrations of Fe^{2+} and H_2O_2 in the mixed solution were 20 mmol/L and 100 mmol/L,
179 respectively. The oxidation process was conducted at a temperature of 30°C , and a stirring
180 rate of 200 rpm for 24 hours. After oxidation, the pH and the concentrations of PAHs in
181 the soil were tested. The results indicated that after oxidative degradation, the pH of soil
182 was 6.49, and the removal efficiency of PAHs was 40.6%. The soil samples were freeze-
183 dried for wheat planting.

184 **Table S1.** Physicochemical properties of the spiked soil and the PAH-contaminated field soil*.

Parameters	Spiked soil	Contaminated field soil
Moisture (%)	2.30	5.20
pH	8.82 ± 0.02	7.08 ± 0.01
Conductivity (mS/m)	9.0 ± 0.1	22.8 ± 0.1
Organic matter (g/kg)	2.4 ± 0.1	10.3 ± 0.11
Total nitrogen (mg/kg)	260 ± 10	260 ± 10
Total phosphorus (mg/kg)	582 ± 3	544 ± 3
Sand particles, 0.05–2 mm (%)	32.4	25.2
Powder particles, 0.002–0.05 mm (%)	66.5	55.0
Clay particles, ≤0.002 mm (%)	1.10	15.2

185 *The contaminated field soil was sampled from an abandoned coking plant site located in the Anhui
 186 Prov., China.

Table S2. Initial concentrations of PAHs and dosage of Tween-80 in liquid medium.

PAHs	Spiked concentrations of PAHs (mg/L)	Dosage of Tween-80 (g/L)
Naphthalene(Nap)	100	5
Phenanthrene (Phe)	100	5
Fluoranthene (Flu)	100	10
Pyrene (Pyr)	100	10
Benzo[a]anthracene (BaA)	100	15
Benzo[b]fluoranthene (BbF)	100	15
Benzo[b]pyrene (BaP)	10	1.5
Dibenz[a,h]anthracene (DBahA)	10	1.5

Table S3 Initial concentrations of PAHs in the contaminated field soil*.

PAHs	Concentrations (mg/kg)		
	Soil A	Soil B	
LMW-PAHs	Naphthalene (Nap)	0.65	0.00
	Phenanthrene (Phe)	0.05	0.20
	Anthracene (Ant)	1.29	0.00
	Other LMW-PAHs	3.16	0.00
HMW-PAHs	Fluoranthene (Flu)	8.59	0.40
	Pyrene (Pyr)	8.21	0.30
	Benzo[a]anthracene (BaA)	10.35	15.30
	Benzo[b]fluoranthene (BbF)	7.06	22.60
	Benzo[a]pyrene (BaP)	2.25	7.20
	Dibenz[a,h]anthracene	3.86	0.00
	Other HMW-PAHs	12.04	1.70
Σ PAHs	57.51	47.70	

190 *Soil A was sampled from an abandoned coking plant site located in Anhui, China, and was used for
191 the lab-scale slurry bioreactor experiments. Soil B was sampled from an abandoned coking plant site
192 located in Tianjin, China, and was used for the pilot-scale slurry bioreactors experiments.

Table S4. Detected intermediates of PAHs in the bioremediation process.

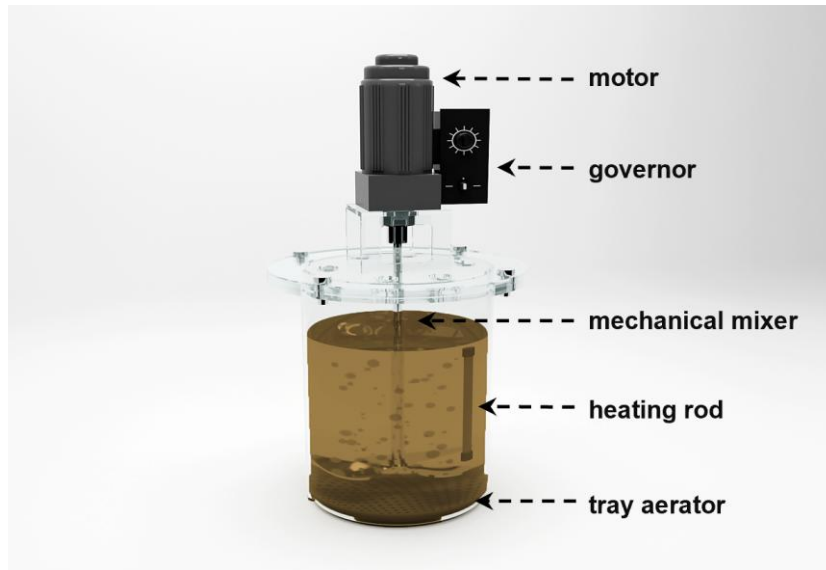
Substrate	Possible metabolites	Formula	Mass	Detection Methods
Naphthalene (Nap)	Salicylic Acid	C ₇ H ₆ O ₃	138.03	LCHRMS
Phenanthrene (Phe)	3,4-Dihydroxybenzoic Acid	C ₇ H ₆ O ₄	154.03	GC-MS
	Salicylic Acid	C ₇ H ₆ O ₃	138.03	LCHRMS
Fluoranthene (Flu)	Salicylic Acid	C ₇ H ₆ O ₃	138.03	LCHRMS
	Catechol	C ₆ H ₆ O ₂	110.04	GC-MS
Pyrene (Pyr)	Salicylic Acid	C ₇ H ₆ O ₃	138.03	LCHRMS
	3,4-Dihydroxybenzoic Acid	C ₇ H ₆ O ₄	154.03	LCHRMS
	Catechol	C ₆ H ₆ O ₂	110.04	GC-MS
Benzo[a]anthracene (BaA)	Salicylic Acid	C ₇ H ₆ O ₃	138.03	LCHRMS
	3,4-Dihydroxybenzoic Acid	C ₇ H ₆ O ₄	154.03	LCHRMS
Benzo[a]pyrene (BaP)	Salicylic Acid	C ₇ H ₆ O ₃	138.03	LCHRMS

Table S5. Comparison of this study with the literatures concerning bioremediation of PAHs in liquid media with Tween-80.

Genus name	Concentration of Tween-80	Concentration of PAHs	Removal efficiency of PAHs	References
<i>Sphingomonas</i> sp.	393 mg/L (0.3 mM)	50 mg/L Ant	89.6% of Ant on 96 hours.	(Al Farraj et al., 2021)
<i>Klebsiella oxytoca</i>	13.1 mg/L	0.12 mg/L Pyr	95% of Pyr on day 18.	(Zhang and Zhu, 2012)
<i>Pseudomonas aeruginosa</i>	160 mg/L	100 mg/L Pyr	98.9% of Pyr on 168 hours.	(Ghosh and Mukherji, 2016)
<i>Burkholderia cepacia</i>	500 mg/L	100 mg/L Pyr.	50% of Pyr on 80 hours.	(Chen et al., 2013)
<i>Phanerochaete sordida</i>	2 g/L	50 mg/L BaP	53.3% of BaP on day 32.	(Li et al., 2023)
<i>Pseudomonas aeruginosa</i>	256 mg/L	50 mg/L BaP	79.7% of BaP on day 25.	(Meng et al., 2019)
<i>Pseudomonas aeruginosa</i> DH-6	0.5-50 g/L	100 mg/L of Nap, Phe, Flu and Pyr; 10 mg/L of BaP and DBahA, respectively.	78.5-99.3% for each PAH on day 7.	This study

Table S6. Comparison of this study with the literatures concerning the bioremediation of PAH-contaminated field soil with Tween-80.

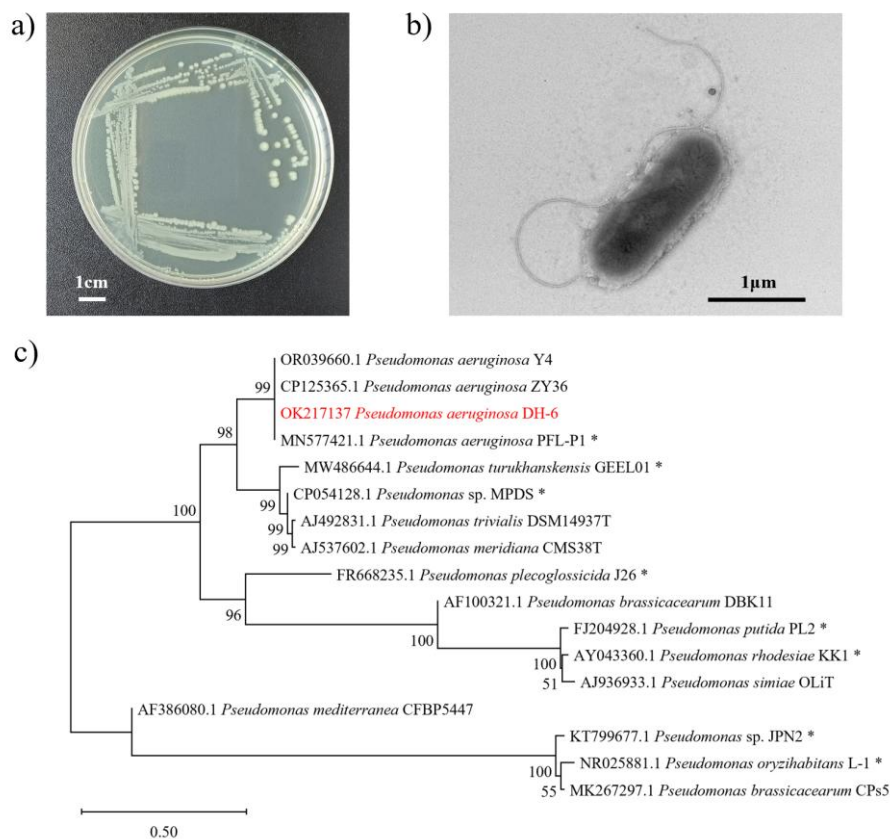
Genus name	Soil type	Concentration of Tween-80	Liquid /soil ratio	Concentration of PAHs	Extraction of PAHs	Removal efficiency of PAHs	References
<i>Klebsiella</i> sp.	Spiked soil	25 g/kg	10:1 v/w	200 mg/kg of Phe, Fla, and Pyr, respectively.	56.4 - 82.7% for each PAHs.	89.1% of Phe, 81.3% of Fla, and 78.3% of Pyr on day 30.	(Xu et al., 2019)
Bacterial consortium	Spiked soil	150 g/kg	30:1 v/w	500 mg/kg of Phe.	93.7% of Phe	74.4% of Phe on day 7.	(Gharibzadeh et al., 2016)
<i>Lasiodiplodia theobromae</i>	Spiked soil	5 g/kg	10:1 v/w	50 mg/kg BaP.	--	32.1 % of BaP on day 35.	(Wang et al., 2014)
<i>Lasiodiplodia theobromae</i>	Field soil	5 g/kg	10:1 v/w	91.4 mg/kg of 16 US EPA PAHs.	--	73.2 % of Σ PAHs on day 30.	(Wang et al., 2014)
<i>Mycobacterium</i> sp.	Field soil	25-50 g/kg	10:1 v/w	258 mg/kg of 16 US EPA PAHs.	9.1% of Σ PAHs	62.4 % of Σ PAHs on day 30.	(Gong et al., 2015)
<i>Pseudomonas aeruginosa</i>	Field soil	25 g/kg	2:1 v/w	57.51 mg/kg of 16 US EPA PAHs.	63.6% of Σ PAHs	88.1% of Σ PAHs, 80.5 - 99.4% of HMW-PAHs on day 14.	This study



199

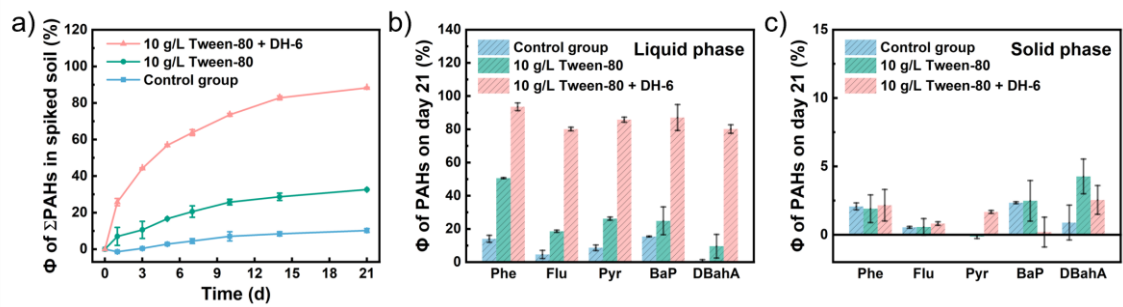
200 **Fig. S1.** The lab-scale slurry bioreactor used in this study. The bioreactor includes a mechanical mixer
201 with impeller-type blades, a motor, a governor, a heating rod, and a tray aerator located at the bottom.

202



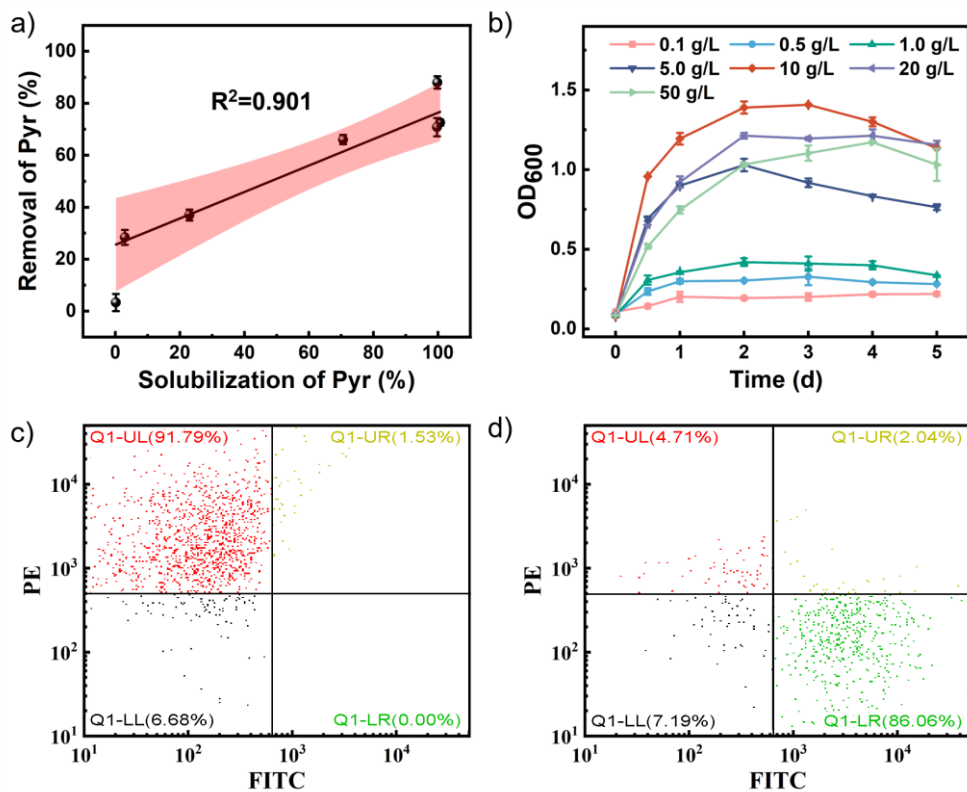
203

204 **Fig. S2.** (a) Appearance of the formed colonies, (b) TEM image of strain DH-6, and (c) phylogenetic
 205 relationships of strain DH-6. *Pseudomonas* isolates known to degrade PAHs are indicated with an
 206 asterisk (*).



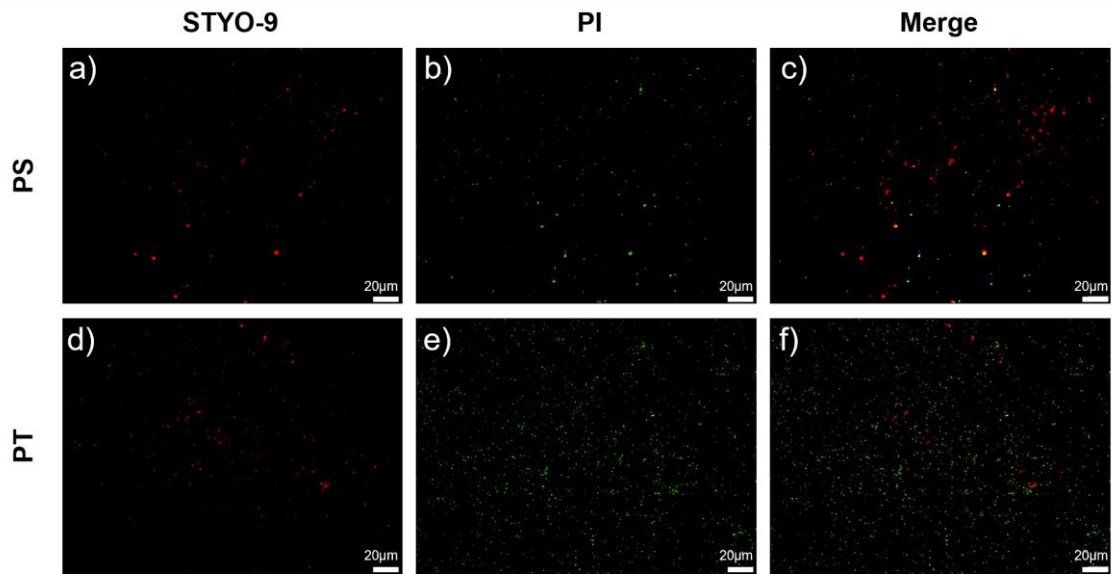
207

208 **Fig. S3.** Removal efficiency of (a) Σ PAHs and five spiked PAHs in (b) liquid phase and (c) solid phase
 209 on day 21. The initial concentration of Σ PAHs in the spiked soil was set at 200 mg/kg, including 60
 210 mg/kg of Phe, 60 mg/kg of Flu, 60 mg/kg of Pyr, 10 mg/kg of BaP, and 10 mg/kg of DBahA. The
 211 water-soil mass ratio of the slurry bioreactor was maintained at 2:1, with 10 g/L Tween-80 added to
 212 the liquid phase. The symbol “ Φ ” represents the removal efficiency.



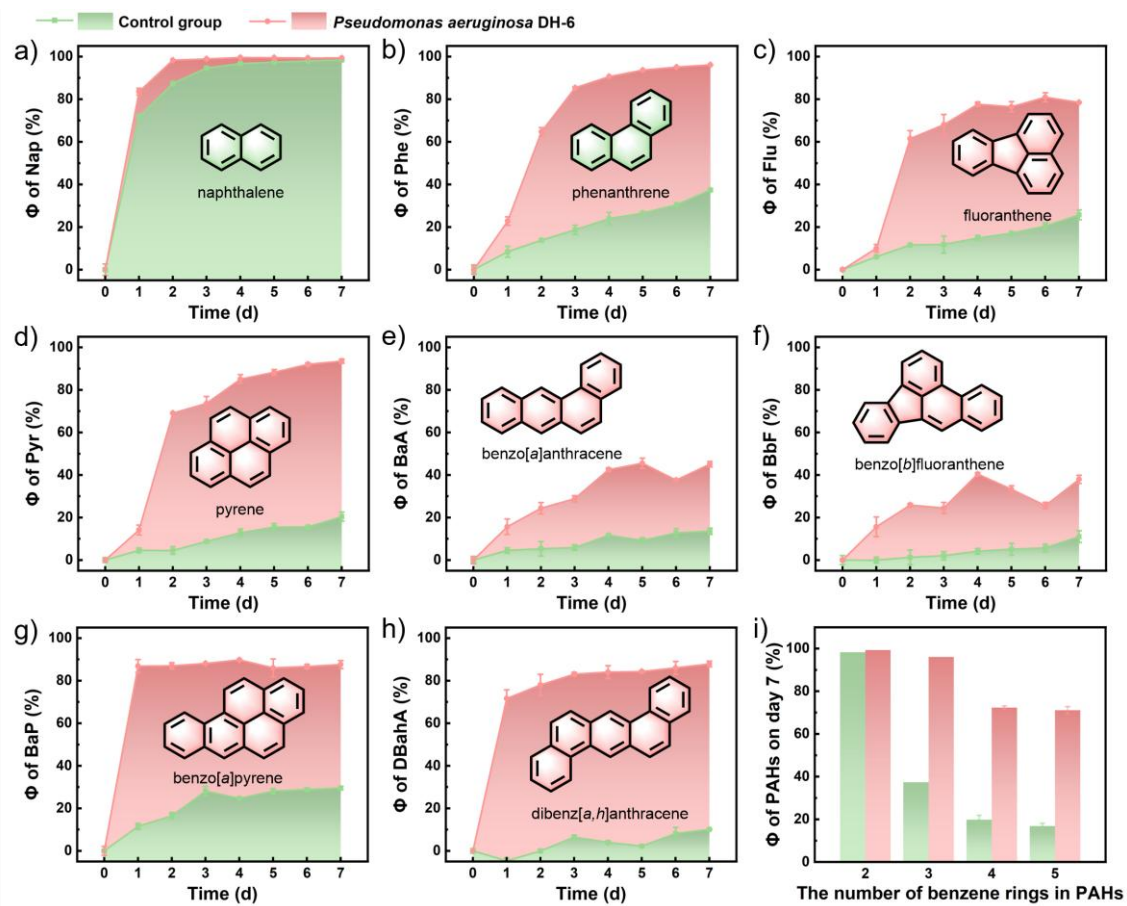
213

214 **Fig. S4.** (a) Linear relationship between the solubilization of Pyr and its removal efficiency. (b) OD₆₀₀
 215 of strain DH-6 in the MSM supplemented with 100 mg/L of Pyr and different concentrations of Tween-
 216 80. Flow cytometry (FCM) analysis of strain DH-6 in PS (c) and PT (d) during the logarithmic growth
 217 phase (36 h). PS: MSM supplemented with Pyr as the sole carbon source. PT: MSM supplemented
 218 with Pyr and 10 g/L Tween-80. STYO9/PI fluorescence dyes were used to differentiate between live
 219 and dead bacteria. Q1-LR represents live bacteria, Q1-UL represents dead bacteria, Q1-LL represents
 220 impurities, and Q1-UR represents damaged bacteria.



221

222 **Fig. S5.** Results of the microbial activity analysis on strain DH-6 in PS (a-c) and PT (d-f) during the
 223 logarithmic growth phase (36 h). PS: MSM supplemented with Pyr as the sole carbon source. PT:
 224 MSM supplemented with Pyr and 10 g/L Tween-80. Visualized using SYTO-9 to stain live biofilm
 225 cells green and PI to stain dead cells red, were examined by fluorescence microscopy.

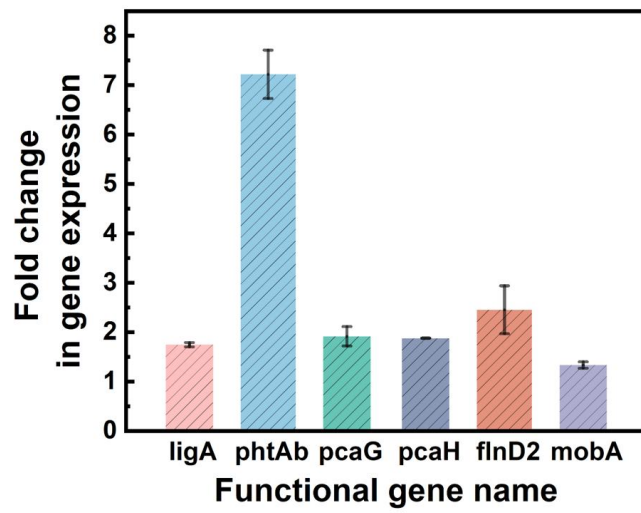


226

227 **Fig. S6.** Removal efficiency of (a) Nap, (b) Phe, (c) Flu, (d) Pyr, (e) BaA, (f) BbF, (g) BaP, (h) DBahA

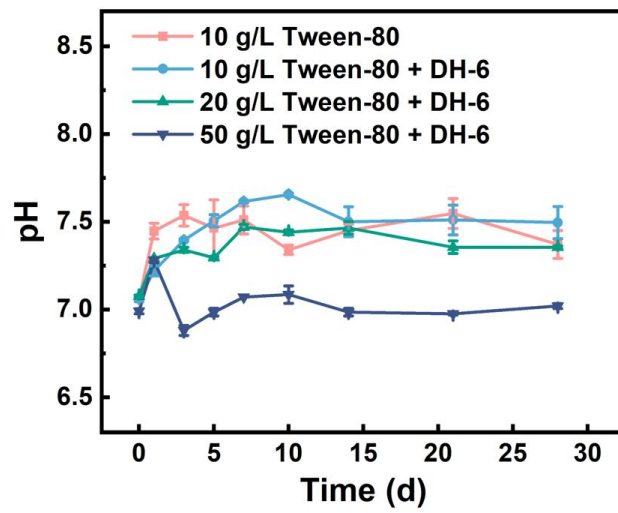
228 in the MSM treated with DH-6, and (i) average removal efficiencies of PAHs on day 7. The symbol

229 “Φ” represents removal efficiency.



230

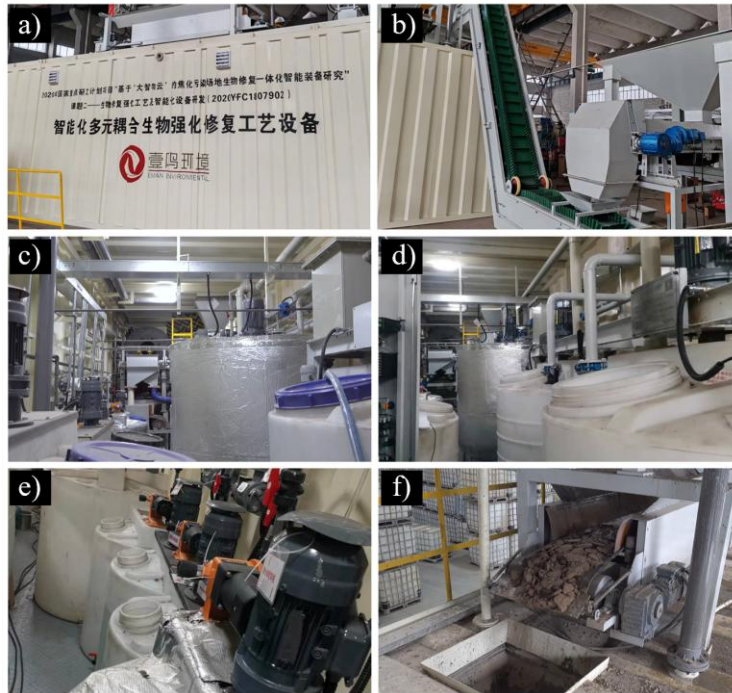
231 **Fig. S7.** QPCR of functional genes related to degrading PAHs in strain DH-6. Experience group: MSM
232 supplemented with 10 g/L Tween-80 and 100 mg/L Pyr; control group: MSM supplemented with 10
233 g/L Tween-80.



234

235 **Fig. S8.** pH variations for the contaminated field soils that were subjected to different experimental

236 treatments.



237

238 **Fig. S9.** The pilot-scale equipment for the experiments on contaminated field soil. (a) Container of
 239 the pilot-scale equipment. (b) In-feed conveyor. (c) Slurry bioreactor. (d) Reactor for oxidation. (e)
 240 Microbial agent barrels and chemicals barrels. (f) Out-feed conveyor.

241

242 References

- 243 Al Farraj, D.A., Alkufeidy, R.M., Alkubaisi, N.A., Alshammari, M.K., 2021. Polynuclear aromatic a
244 ntracene biodegradation by psychrophilic *Sphingomonas* sp., cultivated with tween-80. *Chemos*
245 *phere* 263, 128115. <https://doi.org/10.1016/j.chemosphere.2020.128115>.
- 246 Chen, K., Zhu, Q., Qian, Y., Song, Y., Yao, J., Choi, M.M.F., 2013. Microcalorimetric investigation
247 of the effect of non-ionic surfactant on biodegradation of pyrene by PAH-degrading bacteria *Bu*
248 *rkholderia cepacia*. *Ecotoxicol. Environ. Saf.* 98, 361-367. [https://doi.org/10.1016/j.ecoenv.2013.](https://doi.org/10.1016/j.ecoenv.2013.08.012)
249 [08.012](https://doi.org/10.1016/j.ecoenv.2013.08.012).
- 250 Gharibzadeh, F., Rezaei Kalantary, R., Nasser, S., Esrafil, A., Azari, A., 2016. Reuse of polycyclic
251 aromatic hydrocarbons (PAHs) contaminated soil washing effluent by bioaugmentation/biostimul
252 ation process. *Sep. Purif. Technol.* 168, 248-256. <https://doi.org/10.1016/j.seppur.2016.05.022>.
- 253 Ghosh, I., Mukherji, S., 2016. Diverse effect of surfactants on pyrene biodegradation by a *Pseudomo*
254 *nas* strain utilizing pyrene by cell surface hydrophobicity induction. *Int. Biodeterior. Biodegrad.*
255 108, 67-75. <https://doi.org/10.1016/j.ibiod.2015.12.010>.
- 256 Gong, X., Xu, X., Gong, Z., Li, X., Jia, C., Guo, M., Li, H., 2015. Remediation of PAH-contaminat
257 ed soil at a gas manufacturing plant by a combined two-phase partition system washing and mi
258 crobial degradation process. *Environ. Sci. Pollut. Res.* 22(16), 12001-12010. [https://doi.org/10.10](https://doi.org/10.1007/s11356-015-4466-y)
259 [07/s11356-015-4466-y](https://doi.org/10.1007/s11356-015-4466-y).
- 260 Li, Q., Wang, J., Wang, Z., Zhang, W., Zhan, H., Xiao, T., Yu, X., Zheng, Y., 2023. Surfactants dou
261 ble the biodegradation rate of persistent polycyclic aromatic hydrocarbons (PAHs) by a white-ro
262 t fungus *Phanerochaete sordida*. *Environ. Earth Sci.* 82(12). [https://doi.org/10.1007/s12665-023-1](https://doi.org/10.1007/s12665-023-10970-8)
263 [0970-8](https://doi.org/10.1007/s12665-023-10970-8).
- 264 Meng, L., Li, W., Bao, M., Sun, P., 2019. Effect of surfactants on the solubilization, sorption and bi
265 odegradation of benzo (a) pyrene by *Pseudomonas aeruginosa* BT-1. *J. Taiwan Inst. Chem. En*
266 *g.* 96, 121-130. <https://doi.org/10.1016/j.jtice.2019.01.007>.
- 267 Wang, C., Liu, H., Li, J., Sun, H., 2014. Degradation of PAHs in soil by *Lasiodiplodia theobromae*
268 and enhanced benzo[a]pyrene degradation by the addition of Tween-80. *Environ. Sci. Pollut. Re*
269 *s.* 21(18), 10614-10625. <https://doi.org/10.1007/s11356-014-3050-1>.
- 270 Xu, X., Zhou, H., Chen, X., Wang, B., Jin, Z., Ji, F., 2019. Biodegradation potential of polycyclic ar
271 omatic hydrocarbons by immobilized *Klebsiella* sp. in soil washing effluent. *Chemosphere* 223,
272 140-147. <https://doi.org/10.1016/j.chemosphere.2019.01.196>.
- 273 Zhang, D., Zhu, L., 2012. Effects of Tween 80 on the removal, sorption and biodegradation of pyre
274 ne by *Klebsiella oxytoca* PYR-1. *Environ. Pollut.* 164, 169-174. [https://doi.org/10.1016/j.envpol.](https://doi.org/10.1016/j.envpol.2012.01.036)
275 [2012.01.036](https://doi.org/10.1016/j.envpol.2012.01.036).
- 276